Human Recombinant Phosphodiesterase 4B2B Binds (*R*)-Rolipram at a Single Site with Two Affinities

Warren J. Rocque,*,‡ Gaochao Tian,‡ Jeffrey S. Wiseman, William D. Holmes, Irene Zajac-Thompson, Derril H. Willard, Indravaden R. Patel, G. Bruce Wisely, William C. Clay, Sue H. Kadwell, Christine R. Hoffman, and Michael A. Luther

Department of Biochemistry, Glaxo Wellcome Research Institute, Research Triangle Park, North Carolina 27709

Received May 13, 1997; Revised Manuscript Received August 29, 1997[⊗]

ABSTRACT: The interactions between (*R*)-rolipram and purified human recombinant low-K_m, cAMP-specific phosphodiesterase (HSPDE4B2B) constructs were investigated using biochemical, kinetic, and biophysical approaches. The full-length protein (amino acids 1−564) and an N-terminal truncated protein (amino acids 81−564) exhibited high-affinity (*R*)-rolipram binding, whereas an N-terminal and C-terminal truncated protein (amino acids 152−528) lacked high-affinity (*R*)-rolipram binding. The 152−528 and 81−564 proteins had similar K_m's and k_{cat}/K_m's and differed less than 4-fold compared with the 1−564 protein. (*R*)-Rolipram inhibition plots were biphasic for the 1−564 and 81−564 proteins and fit to two states, a high-affinity (K_i = 5−10 nM) state and a low-affinity (K_i = 200−400 nM) state, whereas the 152−528 protein fit to a single state (K_i = 350−400 nM). The stoichiometry for high-affinity binding using a filter binding assay was found to be <1 mol of (*R*)-rolipram per mole of 1−564 or 81−564 protein. Titration microcalorimetric studies revealed both a high-affinity state with a stoichiometry of 0.3 mol of (*R*)-rolipram per mole of protein and a low-affinity state with a stoichiometry of 0.6 mol of (*R*)-rolipram per mole of protein for the 81−564 protein. A single low-affinity state with a stoichiometry of 0.9 mol of (*R*)-rolipram per mole of protein was seen using the 152−528 protein. The data indicate that purified HSPDE4B2B 1−564 and 81−564 proteins contain a single binding site for (*R*)-rolipram and suggest that the proteins exist in two different states distinguishable by their affinity for (*R*)-rolipram. Furthermore, the high-affinity binding state of the protein requires amino acid residues at the N-terminus (81−151) of the protein and catalytic domain (152−528), whereas the low-affinity binding state only requires residues in the catalytic domain (152−528). Phosphorylation at residues 487 and 489 of the 81−564 protein does not appear to alter the substrate kinetics or the stoichiometry and binding affinity of (*R*)-rolipram.

Phosphodiesterases (PDEs)[1] catalyze hydrolysis of the 3′-phosphoester bond of cyclic nucleotides, such as cAMP, to produce a nucleotide 5′-monophosphate. The effect of increasing levels of cAMP has been linked to airway smooth muscle relaxation (Torphy & Hay, 1990; Torphy & Undem, 1991) and a decrease in inflammatory cell activation (Bourne et al., 1974; Torphy & Undem, 1991). Thus, inhibitors of PDE activity could potentially be used as bronchodilators or anti-inflammatory agents (Torphy & Undem, 1991).

At least seven different mammalian PDE isozymes (Types 1−7) have been identified, each having distinct biochemical and physiological properties (Beavo, 1988; Beavo & Reifsnyder, 1990; Michaeli et al., 1993). The Type 4 PDE, which exists in four isoforms (Bolger et al., 1993) and is characterized by a low K_m for cAMP, is the primary PDE isozyme found in bronchial smooth muscle and inflammatory cells (Silver et al., 1988; Nicholson et al., 1990; Torphy & Cieslinski, 1990; Torphy & Undem, 1991), and is, therefore, an important target of inhibition for the treatment of asthma.

An isozyme-selective inhibitor of Type 4 PDE that is well documented in the literature is rolipram. This inhibitor has been shown to bind to rat brain homogenates stereoselectively and with high-affinity (K_d = 1 nM; Schneider et al., 1986), but it appears to only inhibit Type 4 PDE activity at much higher concentrations (K_i = 1 μM). The effective therapeutic concentrations of rolipram in vivo are, however, very similar to the apparent K_d of the observed high-affinity (*R*)-rolipram binding and not to the apparent K_i of enzyme inhibition (Bolger et al., 1993). Previous studies using (*R*)-rolipram revealed that some Type 4 PDE enzyme preparations exhibit a competitive inhibition pattern suggesting inhibition at the catalytic site (Nemoz et al., 1989; Livi et al., 1990), whereas other enzyme preparations have complex inhibitory kinetics (Torphy et al., 1992; Bolger et al., 1993; McLaughlin et al., 1993; Amegadzie et al., 1995), suggesting the presence of multiple binding forms of PDE. To determine whether PDE 4 has an intrinsic high-affinity for rolipram, Torphy et al. (1992) expressed a human recombinant monocytic Type 4 PDE in yeast cells and determined that high-affinity rolipram binding and cAMP turnover were coexpressed. In addition, other investigators have now linked this high-affinity rolipram binding to other cloned and expressed Type 4 PDE isoforms (Torphy et al., 1992; McLaughlin et al., 1993; Pillai et al., 1993; Amegadzie et

* To whom correspondence should be addressed at Glaxo Wellcome Inc., Five Moore Dr., Research Triangle Park, NC 27709. Phone: (919) 483-3106. Fax: (919) 483-4320.

‡ These authors contributed equally to this paper.

⊗ Abstract published in *Advance ACS Abstracts,* October 15, 1997.

[1] Abbreviations: PDEs, phosphodiesterases; Type 4 PDE, low-K_m cAMP rolipram sensitive PDE; HSPDE4B2B, human recombinant Type 4 PDE isoform B; DPDE and DPD, dunce-like PDE; Sf9, *Spodoptera frugiperda*; T. ni, *Trichoplusia ni*; MOI, multiplicity of infection; HEPES, 4-(2-hydroxyethyl)-1-piperazineethanesulfonic acid; EGTA, [ethylenebis(oxyethylenenitrilo)]tetraacetic acid.

S0006-2960(97)01112-4 CCC: $14.00

al., 1995; Rocque et al., 1997; this manuscript). It is therefore curious how an inhibitor can bind to Type 4 PDEs with high-affinity and have a comparable in vivo effect, yet the enzymatic activity is inhibited only at much higher levels.

One explanation for the discrepancy between the behaviors of rolipram in vitro and in vivo may be that the inhibition of Type 4 PDE enzymatic activity is not necessary to produce the therapeutic anti-depressant action (Torphy et al., 1992), and only the interaction of the high-affinity form of the enzyme expresses the observed biochemical effects. This explanation is not satisfactory considering that the only known function of PDE is its enzymatic activity. Recently, HSPDE4B2B, expressed and purified from baculovirus-infected Sf9 cells, was found to be monophosphorylated on residue 487 and diphosphorylated on residues 487 and 489 (Lenhard et al., 1996). This finding is significant because this differential phosphorylation could offer a structural basis for the presence of high- and low-affinity rolipram binding. But this does not address directly how the phosphorylated states correlate with the different binding affinities and catalytic activities. One major reason for the poor understanding is that the stoichiometry for the interaction between rolipram and PDE has not been resolved unambiguously. Depending upon the stoichiometry, the low and high binding affinities may be assigned either to two different forms of the enzyme or to two binding sites per enzyme molecule. The resolution of this issue is not only fundamental to the understanding of the kinetic and thermodynamic properties of rolipram−PDE interactions in vitro but also crucial to the understanding of the effects of rolipram in vivo. Recently, Jacobitz et al. (1996) report that high-affinity rolipram binding to HSPDE4A is not at an allosteric site but suggest that amino acids outside the catalytic domain may form a high-affinity binding site. Alternatively, they suggest the amino acids outside the catalytic domain may be required for the enzyme to assume a conformation that binds rolipram with high-affinity at the catalytic site.

To further evaluate high-affinity rolipram binding to Type 4 PDE, we have overexpressed in Sf9 and T. ni insect cells and purified to homogeneity an isoform of Type 4 PDE, HSPDE4B2B (McLaughlin et al., 1993; Obernolte et al., 1993), and deletion and point mutants of this enzyme. Using the purified enzymes, we have determined the stoichiometry of (*R*)-rolipram binding using several binding assays, and have characterized the proteins with respect to their biochemical, thermodynamic, and kinetic properties. As will be shown, these studies have led to the conclusion that (1) HSPDE4B2B has a single binding site for (*R*)-rolipram, (2) HSPDE4B2B exists in both a high- and a low-affinity binding state for rolipram binding, (3) amino acid residues in the N-terminal domain (81−151) and catalytic domain (152−528) are critical for high-affinity rolipram binding.

EXPERIMENTAL PROCEDURES

Materials. [2,8-^{3}H]cAMP and [8-^{14}C]adenosine were purchased from DuPont−New England Nuclear. (*R*)-[^{3}H]-Rolipram (82 Ci/mmol) was prepared by Dr. Shimoga Prakash (Glaxo Wellcome Research Institute, Research Triangle Park, NC). (*R*)-Rolipram was synthesized at Glaxo Wellcome Research Institute, Research Triangle Park, NC. Other reagents purchased were as follows: M13 from New England Biolabs Inc.; cation liposome transfection kit from Invitrogen; Grace's media, gentamycin, and Sf900II media from Gibco; lactalbumin hydrolysate and yeastolate from Difco; fetal bovine serum from Hyclone Laboratories; Sf9 cells from the ATCC; Bradford protein dye from Pierce Chemical Co.; Q-Sepharose Fast Flow resin, Superdex-200 column resin, and QAE-Sephadex from Pharmacia; hydroxyapatite column from Koken; 96-well filter plates from Millipore; 96 well microtiter plates from Costar; 96-well microbeta scintillation plates and Optiphase 'High Safe' 3 scintillation fluid from Wallac; microdialyzer and equilibrium dialysis membranes from Hoeffer Scientific; hydroxyapatite for rolipram binding experiments from BioRad; bovine serum albumin from Boehringer Mannheim; Bellco bottle bioreactors from Bellco; Centriprep concentrators from Amicon; Poros Q media from Perseptive Biosystems; Cibacron Blue-300 resin, nucleotidase, and all other chemicals at the highest grade from Sigma

Generation of HSPDE4B2B Constructs in Baculovirus. HSPDE4B2B is a 564 amino acid protein (McLaughlin et al., 1993; Obernolte et al., 1993). The following list represents the amino acid residues (in parentheses) of the truncations and site-directed mutants of HSPDE4B2B that were constructed and expressed using a baculovirus expression system. HSPDE4B2B 81−564 (81−564); HSPDE4B2B 81−564 with serine to alanine mutations at residues 482, 487, and 489 (81−564 SΔA); HSPDE4B2B 152−528 (152−528); and HSPDE4B2B 152−528 with serine to alanine mutations at residues 482, 487, and 489 (152−528 SΔA). These constructs were generated as previously described (Lenhard et al., 1996; Rocque et al., 1997) using standard baculovirus techniques (O'Reilly et al., 1992; Summers & Smith, 1987). HSPDE4B2B 81−564 and 152−528 proteins were expressed in Sf9 cells using SF900ll media. All other constructs were expressed in T. ni 5B14 cells using Excell 405 media. Optimal growth conditions for obtaining a large quantity of protein were determined for baculovirus expression by varying the harvest time and the multiplicity of infection (MOI). Purified HSPDE4B2B 1−564 (1−564) was supplied as a kind gift from Drs. Tim Martins and Vince Florio from the ICOS Corp., Bothell, WA.

Purification of HSPDE4B2B Constructs. HSPDE4B2B 152−528 and 152−528 SΔA were purified using a four column step procedure; HSPDE4B2B 81−564 and 81−564 SΔA were purified using a five column step procedure (Lenhard et al., 1996; Rocque et al., 1997). All samples were quality-controlled for molecular weight, purity, and protein concentration by electrospray ionization mass spectrometry, Edman sequencing, SDS−polyacrylamide gel electrophoresis, and quantitative amino acid analysis. Each HSPDE4B2B protein was >95% homogeneous.

PDE Activity Assays. All the activity assays were performed at 22 °C using the following assay buffer: 2 mM Tris-HCl, pH 7.5, 1 mM $MgCl_2$, 0.2 mM EDTA, 0.2 mM DTT, 0.5 mg/mL BSA, 0.05% *n*-octyl glucoside, 15 nM aprotinin, 200 nM leupeptin, 100 μM pefabloc A, 1 μg/mL soybean trypsin inhibitor, 100 μM benzamidine, 13 μM bestatin, 0.1 μg/mL pepstatin A, and 0.2 μg/mL calpain. To a well of a 96-microwell plate were added 60 μL of a 1.67× concentrated assay buffer, 10 μL of 1× buffer, and 10 μL of a mixture of 0.3 μL of [^{3}H]cAMP (1 μCi/μL) and 1.5 μL of [^{14}C]adenosine (0.02 μCi/μL). This mixture was incubated at 22 °C for 15−20 min. To initiate the reaction, 20 μL of an enzyme mixture containg 10 μL of 5′-nucleotidase (100

μg/mL) and 10 μL of PDE was added. The final concentration of cAMP was 94 nM. To stop the reaction, 20 μL of a solution containing 50 mM 3-(cyclohexylamino)-1-propanesulfonic acid (CAPS), pH 10, was added. Following the quench, 80 μL of the reaction mixture was transferred to 200 μL of a 50% slurry of QAE Sephadex in 5 mM CAPS, pH 10, in a filter bottom plate (Millipore, no. MAGVN2250) and vacuum-filtrated. Eighty microliters of the filtrate was transferred to a Pharmacia counting plate and 150 μL of scintillation cocktail added. Samples were counted in a Wallac 1450 microbeta scintillation counter. The ratio of $^3H/^{14}C$ of the filtrate, $(^3H/^{14}C)_{filtrate}$, to $^3H/^{14}C$ of the reaction mixture before addition of enzyme, $(^3H/^{14}C)_o$, was used to calculate the activity by

$$\frac{V}{K} = -\frac{1}{\Delta t} \ln \frac{(^3H/^{14}C)_{filtrate}}{(^3H/^{14}C)_o} \quad (1)$$

where V/K represents the pseudo-first-order rate constant under the condition where $[S] \ll K_m$, and Δt is the assay time.

Time-Dependent Inhibition of PDE by Rolipram. Enzyme assays were run in the presence or absence of 1 μM rolipram under the assay conditions described in the section *PDE Activity Assays*. A 2 mL reaction mixture was made, and an 80 μL aliquot was quenched at different time points ($\leq$60 min). The data for progress curves in the absence of inhibitor were analyzed by

$$\frac{[S]}{S_t} = e^{-(V/K)t} \quad (2)$$

In the case where inhibitor was present, a two-step reversible model:

$$E + I \overset{K_i}{\rightleftharpoons} EI \underset{k_4}{\overset{k_3}{\rightleftharpoons}} EI^* \quad (3)$$

was used to analyze the data, where I is the inhibitor and EI and EI* are enzyme−inhibitor complexes. In this model, the first step is fast, leading to formation of an initial enzyme−inhibitor complex EI. The second step, characterized by the rate constants k_3 and k_4, is responsible for the observed time dependence. The progress curve data were then analyzed according to the equation:

$$\frac{[S]}{S_t} = e^{-\{(V/K)_s t - [[(V/K)_0 - (V/K)_s]/k_{obsd}]e^{-k_{osbd}t}\}} \quad (4)$$

where $(V/K)_0$ and $(V/K)_s$ represent, respectively, the PDE activities at $t = 0$ and after the time-dependent event, and k_{obsd} is the observed inhibition rate constant given by

$$k_{obsd} = \frac{k_3[I]}{K_i + [I]} + k_4 \quad (5)$$

Inhibition Kinetics. The inhibition experiments were carried out as described under *PDE Activity Assays* except in the presence of (*R*)-rolipram at defined concentrations. (*R*)-Rolipram was prepared in 10% dimethyl sulfoxide (DMSO) and added to the reaction mixture with 10× dilution such that the final DMSO concentration was 1%. We found that DMSO concentrations of 1% did not affect PDE activity. The enzyme was incubated with (*R*)-rolipram for 1 h prior to assaying. The kinetic inhibition data were analyzed by either a one-site (state) or a two-site (two-state) noncoupling model according to the following equations as described by Cleland (1970), respectively:

$$\frac{V}{K} = \frac{(V/K)_o}{1 + [I]/K_i} + b \quad (6)$$

and

$$\frac{V}{K} = \frac{(V/K)_{o(1)}}{1 + [I]/K_{i(1)}} + \frac{(V/K)_{o(2)}}{1 + [I]/K_{i(2)}} + b \quad (7)$$

where $(V/K)_o$ is enzyme activity in the absence of inhibitor, [I] is the concentration of inhibitor, and K_i is the inhibition constant. In eqs 6 and 7, b represents the background and the subscripts 1 and 2 are designated for sites (states) 1 and 2, respectively.

Job-Plot Filter Binding Assays. All the assays were conducted in 2 mM Tris-HCl, pH 7.5, containing 0.2 mM DTT, 0.2 mM EDTA, 1 mM $MgCl_2$, and 0.5 mg/mL BSA. Glass fiber filter mats were pretreated with 0.3% polyethylenimine (PEI) for 2 h and dried before use. [^{3}H]-(*R*)-Rolipram was prepared as follows. A solution of [^{3}H]-(*R*)-rolipram estimated at 200 nM was prepared in the Tris buffer containing 1% DMSO. The actual (*R*)-rolipram concentration was then determined by measuring the radioactivity of the solution against a tritium standard and by using the known specific activity (82 Ci/mmol) of the [^{3}H]-(*R*)-rolipram. Stock solutions of the different HSPDE4B2B constructs were then prepared at the same concentration as the [^{3}H]-(*R*)-rolipram solution. The [^{3}H]-(*R*)-rolipram and enzyme solutions with various molar fractions, but at a constant sum of enzyme and ligand, were then mixed in a 96-well plate. The mixtures were allowed to stand at room temperature (22 °C) for 1 h and then cooled for 15 min on ice before filtration. All of the subsequent steps were performed at 4 °C. A filter mat pretreated with PEI was positioned onto the platform of a Tomtec cell harvester and held tightly with the filter mat clamp. The plate containing binding mixtures was placed under an aspiration manifold with aspiration tips submerged and nearly touching the bottom of the wells. The filtration was then initiated by an automated sequence of aspiration and washing. A 5 s aspiration trapped the enzyme−ligand complex onto the filter mat, and this was followed by a 3.5 s wash with 25 mM Tris-HCl, pH 7.4, containing 100 mM NaCl, to remove the free ligand. The filter was then semi-dried for 15 s with the house vacuum attached to the harvester and subsequently fully air-dried. The dried filter mat was sealed in a plastic scintillation bag with 2 sheets of Meltilex solid scintillant. The plastic scintillation bag was heated on a hot plate at 80 °C until the scintillant was uniformly soaked into the filter mat. The enveloped sheet was placed in a cassette and the radioactivity per well determined in a Wallac 1450 microbeta scintillation counter. The counts (cpm), which are proportional to the amount of enzyme−ligand complex, were plotted against the molar fraction of enzyme, χ_e. The stoichiometry of the binding is given by

$$n = \frac{1 - (\chi_e)_s}{(\chi_e)_s} \quad (8)$$

where (χ_e) corresponds to the value of molar fraction at the highest cpm.

Equilibrium Dialysis. To assess low-affinity (*R*)-rolipram binding, equilibrium dialysis experiments (Klotz et al., 1946) were performed using a Hoeffer Microdialyzer. Experiments were performed by dialyzing 2−6 μM purified HSPDE4B2B 1−564 or 81−564 against increasing concentrations of (*R*)-rolipram; 100 μL of enzyme, in 50 mM HEPES, 250 mM NaCl, and 2.5 mM $MgCl_2$, pH 7.5, was added to one side of a 12−14K molecular weight cutoff membrane, and an equal volume of fixed [^{3}H]-(*R*)-rolipram and varying concentrations of cold (*R*)-rolipram (0.04−30 μM final) were added to the other side in the same buffer with 0.5% DMSO. HSPDE4B2B and (*R*)-rolipram were dialyzed at 4 °C for 20 h. Fifty microliters of sample from the HSPDE4B2B−(*R*)-rolipram side (bound + free ligand) and the same volume from the side without protein (free ligand) were pipetted into separate wells of a 96-well microbeta scintillation plate. Two hundred microliters of Optiphase "High Safe" 3 liquid scintillation fluid was added to each well, and the plates were counted in a Wallac 1050 microbeta scintillation counter (Wallac Inc., Gaithersburg, MD). Dialysis membranes were also counted to determine any nonspecific binding to the membranes. Data were plotted as $[(R)\text{-rolipram}]_{free}$ vs $[(R)\text{-rolipram}]_{bound}/[\text{HSPDE4B2B}]$ and fit by a nonlinear least-squares regression program to obtain the stoichiometry (n) and the equilibrium constant (K_b). Protein concentrations were determined before and after dialysis.

Isothermal Titration Microcalorimetry. The titration of HSPDE4B2B constructs with (*R*)-rolipram was carried out using a MicroCal MCS titration calorimeter (MicroCal Inc., Northhampton, MA). The instrumentation and experimental design for the titration calorimeter have previously been described (Wiseman et al., 1989). (*R*)-Rolipram was dissolved in 50 mM HEPES, 250 mM NaCl, 2 mM $MgCl_2$, and 0.5% DMSO, pH 7.5, and protein was solubilized in the same buffer without DMSO. In a typical experiment, (*R*)-rolipram (100 μM in a 250 μL syringe) was titrated over 25−30 injections of varying volumes (6−12 μL) into purified HSPDE4B2B 81−564, 81−564 SΔA, or 152−528 SΔA (11 μM in the cell) at either 16 or 28 °C. Titrations were performed at 3.5 min intervals at a stirring speed of 600 rpm. The amount of heat due to (*R*)-rolipram binding to HSPDE4B2B constructs was measured by integrating the area of each titration peak. Data analysis and curve fitting were carried out using the Origin software package supplied by Microcal using either a one-site model (for HSPDE4B2B 152−528) or a two independent site model (for HSPDE4B2B 81−564 and 81−564 SΔA). The equations for these models have been previously described (Wiseman et al., 1989; Lin et al., 1991). The heat measured at each titration was corrected for the heat of dilution of (*R*)-rolipram into buffer before data analysis. Protein concentrations were determined by quantitative amino acid analysis.

Analytical Ultracentrifugation. Sedimentation equilibrium analytical ultracentrifugation was performed using a Beckman XL-A centrifuge (Beckman, Fullerton, CA) with two-channel 12 mm charcoal-filled epon centerpieces. Scans were taken at 280 nm at 1 h intervals throughout the run. Runs were performed at 10 000, 12 500, and 15 000 rpm at 4 °C for HSPDE4B2B 81−564, at 10 000, 15 000, and 20 000 rpm at 4 °C for HSPDE4B2B 152−528 proteins, and at 1000, 2000, and 3000 rpm at 4 °C for HSPDE4B2B 1−564. Equilibrium was judged to be achieved by the absence of change between plots of several successive scans after approximately 20 h; 180−200 μL of each sample was centrifuged against 250 μL of equivalent buffer, 50 mM HEPES, 250 mM NaCl, pH 7.5. Protein concentrations used were 0.28 and 2.8 mg/mL for HSPDE4B2B 81−564; 0.09, 0.45, and 0.9 mg/mL for HSPDE4B2B 152−528 SΔA; and 1.7 mg/mL for HSPDE4B2B 1−564. Solvent density was determined empirically at 4 °C using a Mettler DA-110 density, specific gravity meter (Mettler, Highstown, NJ) calibrated against water. The partial specific volume of each protein, ν, was calculated using the method of Cohn and Edsall (1943). The effect of temperature was taken into account using the method of Durschlag (1986), using ν values derived for each amino acid at 25 °C (Laue et al., 1992). Data sets were obtained as radial distance versus absorbance. The raw data were analyzed by a Beckman/Microcal Origin nonlinear regression software package using multiple iterations of the Marquardt−Levenberg algorithm for parameter estimation (Marquardt, 1963). Multiple models were employed to determine the most accurate description of the protein solution state (McRorie & Voelker, 1993). Equilibrium constants (K_a's) obtained from data fitting were converted to molar dissociation constants. These dissociation constants were then used to calculate theoretical concentrations of monomer, dimer, and tetramer species at any given protein concentration (McRorie & Voelker, 1993).

RESULTS

Expression and Protein Purification. Cell lysates of the overexpressed HSPDE4B2B proteins produced high levels of Type 4 PDE activity and (*R*)-rolipram inhibition compared to control cells lacking the HSPDE4B2B construct. The Cibacron blue column was a critical step that typically gave 15−20-fold purification. All of the HSPDE4B2B proteins bound to Cibacron blue resin and could not be eluted with 1.5 M NaCl. High levels of cAMP (≥5 mM) were necessary to elute the enzyme from the column.

The association of other cellular proteins with HSPDE4B2B constructs was also noted during the purification of HSPDE4B2B 1−564 and 81−564. A copurifying protein, determined to be heat shock protein 70 (hsp70), was found in both Sf9 and yeast preparations. The hsp70 and HSPDE4B2B 81−564 protein could only be separated using hydroxylapatite chromatography. Hsp70 was only found in small amounts during the HSPDE4B2B 152−528 purification and could be removed using gel filtration chromatography.

Each protein construct eluted from a Superdex-200 sizing column in a manner consistent with a self-associating species (larger than monomeric). All but the 1−564 protein eluted with molecular masses <200 kDa, suggesting the proteins were no larger than tetramers. The 1−564 protein, however, appeared to exist as a large multimer (molecular mass >600 kDa) and eluted in the exclusion volume of the column. The purified proteins were >95% pure as determined by mass spectrometry, by SDS gels, and by Western blotting against an antibody directed toward the catalytic domain (data not

shown). Mass spectrometric analysis of all of the purified proteins also indicated the correct molecular mass for the nonphosphorylated serine to alanine mutants and a monophosphorylated (Ser 487) and diphosphorylated (Ser 487, 489) species in the proteins with serine residues present (Lenhard et al., 1996). The ratio of monophosphorylated to diphosphorylated protein was approximately 1:1 for each protein.

Enzymatic Activities of HSPDE4B2B Constructs. The K_m for cAMP (2−5 μM) was similar for all HSPDE4B2B constructs tested (data not shown), indicating amino acid residues 1−151 are unimportant for cAMP recognition. Also, k_{cat}/K_m values were similar among the deletion constructs HSPDE4B2B 81−564 and 152−528, and 3−4 times higher than the k_{cat}/K_m value for the HSPDE4B2B 1−564 protein. There were undetectable levels of cGMP hydrolyzing activity (<1% of cAMP activity) found for each of the purified proteins. Mutating serines 482, 487, and 489 to alanine in HSPDE4B2B 81−564 and 152−528, to eliminate phosphorylation of these proteins, had no effect on the specific activity of the purified enzymes or the ability to hydrolyze cGMP. Thus, phosphorylation alone of HSPDE4B2B is apparently not a mechanism for modulating cAMP turnover.

An HSPDE4B2B protein truncated by 151 amino acids at the N-terminus and 86 amino acids at the C-terminus (152−478) was not active when expressed in Sf9 or yeast but was detected on Western blots using an antibody directed toward the HSPDE4B2B catalytic domain. However, a truncation of 151 amino acid residues at the N-terminus and 59 amino acids at the C-terminus (152−505) was completely active when expressed in baculovirus-infected T. ni cells. It is unknown whether this lack of activity of the 152−478 construct was due to the loss of critical catalytic and/or structural amino acid residues. This 152−478 protein lacks the stretch of amino acids at the extreme C-terminus of the catalytic domain that are phosphorylated (residues 479−505; Lenhard et al., 1996). This region (479−505), phosphorylated or not, may be important for maintaining an active conformation for catalysis.

Biphasic and Time-Dependent Inhibition of HSPDE4B2B with (R)-Rolipram. Previous studies have shown that HSPDE4 is inhibited at micromolar concentrations of (*R*)-rolipram, but not inhibited at (*R*)-rolipram concentrations that have been suggested to cause anti-depressant activity (Torphy et al., 1992). However, when examined by filter binding assays, (*R*)-rolipram showed a single K_d value of ∼1 nM for HSPDE4B2B 81−564 (Rocque et al., 1997). In these assays, the lack of a second K_d, corresponding to the low-affinity (micromolar) inhibition of the enzymatic activity, can be ascribed to the likely collapse of the loose inhibitor−enzyme complex during the wash steps. These observations suggest that the enzyme may have two sites or states: one site or state that has the enzymatic activity and is inhibited by (*R*)-rolipram at high concentrations and a second site or state that has no enzymatic activity but can bind the inhibitor with a much greater affinity. Whether the discrepancy between K_i and K_d is due to differences in experimental conditions has not been carefully investigated. Reexamination of the assay conditions for inhibition of enzymatic activity and for binding of the enzyme by (*R*)-rolipram indicated a time difference. The inhibition studies were normally done with a 10−15 min reaction time without preincubation of enzyme and inhibitor, whereas the filter

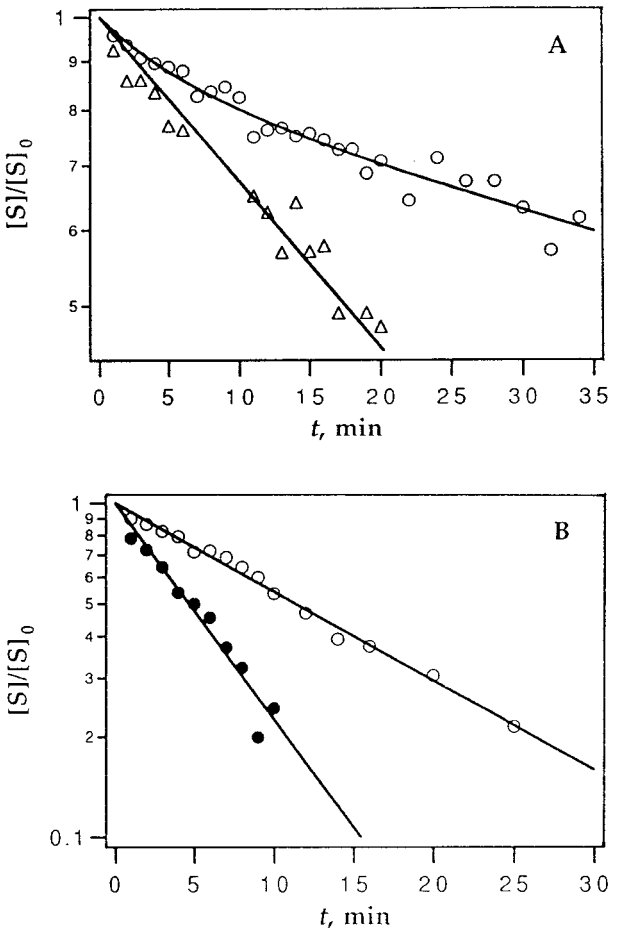

FIGURE 1: Progress curves of the reaction of HSPDE4B2B with (A) 1−564 in the presence (○) or absence (△) of 100 nM (*R*)-rolipram at pH 7.0, 23 °C, and (B) 152−528 in the presence (○) or absence (●) of 100 nM (*R*)-rolipram at pH 7.0, 23 °C. The data in the absence of inhibitor for HSPDE4B2B 1−564 and for 152−528 were fit to eq 2 whereas the data for HSPDE4B2B 1−564 in the presence of inhibitor were fit to eq 4 (see Experimental Procedures).

binding assays used for binding studies were routinely conducted with a 1 h incubation of enzyme and inhibitor prior to filtration and washing. To gain insights into whether the time difference played a role in the apparent difference in the values of K_i and K_d, we conducted a progress curve analysis of enzyme inhibition by (*R*)-rolipram. To our surprise, we found that the inhibition is indeed time-dependent as revealed by the shape of the progress curve (Figure 1). A half-life of about 15 min for the time-dependent inhibition may be estimated by inspection of the progress curve. Based on the time-dependent inhibition exhibited by (*R*)-rolipram, HSPDE4B2B was preincubated with varying concentrations of (*R*)-rolipram for 1 h prior to determining initial velocity rates. Under these conditions, the initial rates were linear with respect to time. (*R*)-Rolipram concentration-dependent inhibition using these conditions showed that HSPDE4B2B 1−564 exhibited two transitions. Analysis of the data according to eqs 6 and 7 (see Experimental Procedures) showed one transition is associated with a K_i of 390 nM corresponding to the low-affinity inhibition site or state observed before with HSPDE4B2B 81−564 (Rocque et al., 1997). The second transition, which has not been described before, has a K_i of 6 nM, similar to the value of the K_d obtained by binding studies of HSPDE4B2B 81−564 (Rocque et al., 1997).

Table 1: Summary of the Inhibition of HSPDE4B2B Constructs by (*R*)-Rolipram

	HSPDE4B2B construct				
kinetics	1−564	81−564	81−564 SΔA	152−528	152−528 SΔA
state/sites	2	2	1	1	1
K_i (nM)	5.6 ± 1.6 390 ± 90	8.6 ± 2.5 240 ± 100	220 ± 30	360 ± 40	400 ± 50
% state 1:% state 2[a]	35:65	50:50	NA[b]	NA	NA

[a] The percent of states was determined by taking *V*/*K* for state 1 and dividing by *V*/*K* for state 2. [b] NA, not applicable.

These results strongly suggest that both sites or states of HSPDE4B2B may have enzymatic activities. HSPDE4B2B 1−564 and 81−564 were both shown to contain this high- and low-affinity inhibitory state (Table 1). In contrast, HSPDE4B2B 152−528 had only one inhibitory state corresponding to the low-affinity site or state (Figure 2). The high-affinity inhibition of the HSPDE4B2B 1−564 and 81−564 proteins was similar to what has been reported for high-affinity (*R*)-rolipram binding with crude lysates of HSPDE4B2B expressed in yeast and insect cells (McLaughlin et al., 1993; Amegadzie et al., 1995).

Binding of (R)-Rolipram to HSPDE4B2B Constructs by a Filter Binding Assay. We have previously shown that [^{3}H]-(*R*)-rolipram binds to HSPDE4B2B 81−564 with high-affinity (1.5 nM) using a filter binding assay, but the observed stoichiometries were <0.1 mol of (*R*)-rolipram per mole of HSPDE4B2B 81−564 (Rocque et al., 1997). To further examine the stoichiometry of high-affinity (*R*)-rolipram binding to other forms of HSPDE4B2B and to determine whether phosphorylation affected this stoichiometry, a different filter binding assay was designed, and the results were analyzed by Job plots (Cantor & Schimmel, 1980). Using equal protein concentrations, both the HSPDE4B2B 81−564 and 1−564 proteins bound (*R*)-rolipram with high-affinity (Figure 3), whereas the 152−528 protein showed very little binding under the same conditions. The stoichiometry of (*R*)-rolipram binding to HSPDE4B2B 1−564 was 0.3 mol of (*R*)-rolipram per mole of protein. The stoichiometry with HSPDE4B2B 81−564 was 0.6 mol of (*R*)-rolipram per mole of protein (Table 2). The stoichiometry reported here for HSPDE4B2B 81−564 was greater than that previously reported (Rocque et al., 1997). This difference is likely due to changes in the assay conditions and methods of analysis.

The stoichiometries reported for HSPDE4B2B 81−564 and 1−564 by the filter binding assay above primarily represent high-affinity binding since the filter binding assay is a nonequilibrium binding method. If the low-affinity binding state of (*R*)-rolipram is a result of a fast off rate, then low-affinity binding may not be readily detected with this assay. Furthermore, the counts detected for high-affinity binding would mask the counts binding at the low-affinity site using this method of analysis. Thus, since [^{3}H]-(*R*)-rolipram bound to HSPDE4B2B 81−564 and 1−564 with high-affinity, a low-affinity [^{3}H]-(*R*)-rolipram site/state could not be readily detected using this method of analysis. In contrast, analysis of the 152−528 protein using the filter binding assay showed 20- and 40-fold lower [^{3}H]-(*R*)-rolipram counts bound compared to the 1−564 and 81−564 proteins, respectively. We attribute these fewer counts bound to the 152−528 protein to low-affinity binding, since these residual counts are no longer masked by high-affinity binding. When the 152−528 data are analyzed by Job plots,

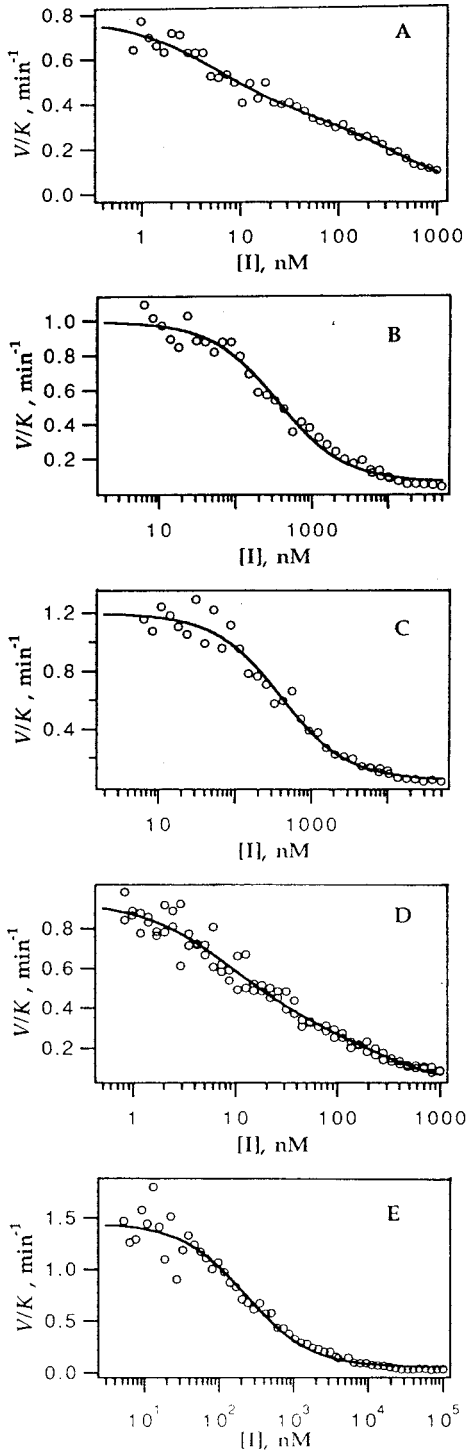

FIGURE 2: Inhibition of HSPDE4B2B constructs (A) 1−564, (B) 152−528, (C) 152−528 SΔA, (D) 81−564, and (E) 81−564 SΔA by (*R*)-rolipram. The data presented in (A) and (D) were analyzed according to eq 7, and data presented in (B), (C), and (E) were analyzed using eq 6 (see Experimental Procedures). The results can be found in Table 1.

Table 2: Summary of (*R*)-Rolipram Binding to HSPDE4B2B Constructs

binding assay	HSPDE4B2B construct				
	1−564	81−564	81−564 SΔA	152−528	152−528 SΔA
filter binding					
stoichiometry (mol of ligand/mol of PDE)	0.3	0.6	1.1	0.9	0.9
equilibrium dialysis					
stoichiometry (mol of ligand/mol of PDE)	0.5	0.74	ND[a]	ND	ND
K_d (nM)	100	140	ND	ND	ND
titration calorimetry					
stoichiometry (mol of ligand/mol of PDE)	ND	0.28/0.55	0.26/0.69	ND	0.92
K_d (nM)	ND	7.1/210	6.1/910	ND	1000

[a] ND, not determined.

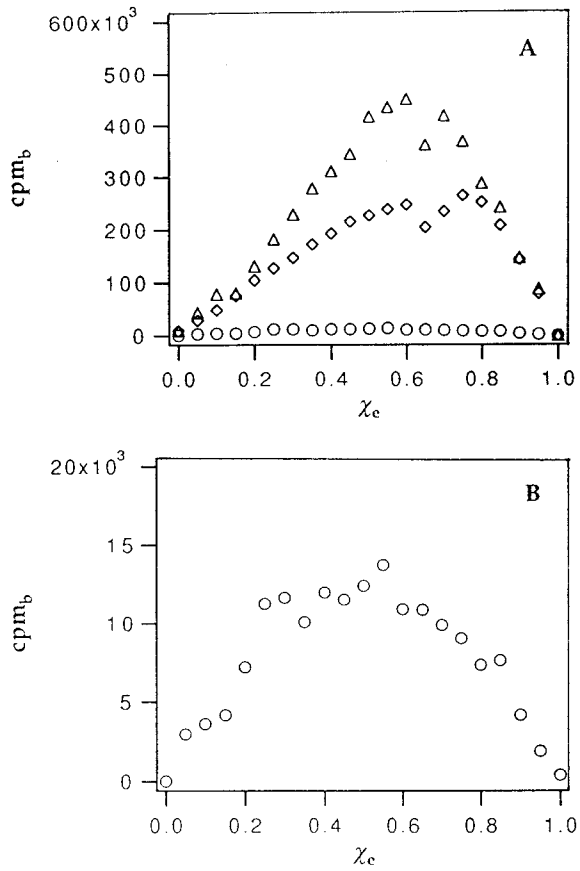

FIGURE 3: Analysis of (*R*)-rolipram−HSPDE4B2B binding stoichiometry using Job plots. (A) The amount of the complex [^{3}H]-(*R*)-rolipram−PDE, in cpm, was plotted vs the mole fraction of protein, χ_e, for 1−564 (◇), 81−564 (△), and 152−528 (○). The total concentration of inhibitor and enzyme was held at 133 nM. (B) An expanded view of the bottom trace, 152−528 (○), shown in part A. χ_e values corresponding to apexes in these plots were used to calculate the stoichiometry values according to eq 8 (Experimental Procedures). To aid in estimating the χ_e values, two linear lines were calculated, one using the early half of the ascending data points and the other using the late half of the descending data points of the same plot. The interception of the two linear lines was equated to the χ_e value. The stoichiometry of (*R*)-rolipram binding to HSPDE4B2B can be found in Table 2.

a stoichiometry of 0.9 mol of (*R*)-rolipram per mole of protein is obtained (Figure 3B). Thus, the outcome of filter binding assays suggests that (*R*)-rolipram binds to HSPDE4B2B 81−564 and 1−564 with high-affinity whereas HSPDE4B2B 152−528 lacks this high-affinity site/state.

Binding of (R)-Rolipram to HSPDE4B2B Constructs by Equilibrium Dialysis. The filter binding technique for determining stoichiometry and ligand affinity is not an equilibrium method; therefore, we designed experiments to measure a more "true" equilibrium binding constant and stoichiometry for (*R*)-rolipram using equilibrium dialysis. In order to obtain adequate signal to noise, high concentrations of HSPDE4B2B proteins (2−5 μM) were necessary. This meant only low-affinity (*R*)-rolipram binding constants could be determined using these assays. We have previously shown that HSPDE4B2B 81−564 had an apparent K_d of 140 nM with a stoichiometry of 0.74 mol of (*R*)-rolipram per mole of HSPDE4B2B 81−564 (Rocque et al., 1997). HSPDE4B2B 1−564 had a stoichiometry of binding of 0.5 mol of (*R*)-rolipram per mole of HSPDE4B2B 1−564 and an apparent K_d of 100 nM (Figure 4). These binding data were consistent with other kinetic and binding experiments in which a low-affinity binding site/state was observed. The data obtained using equilibrium dialysis, however, are important because they suggest the stoichiometry of (*R*)-rolipram binding to be <1, indicating a single binding site on the protein, not two independent sites. However, because of the inability to determine a saturable high-affinity binding constant in constructs that showed high-affinity binding in the filter binding assay, the other HSPDE4B2B constructs were not tested. Instead, a third experimental approach was taken to determine stoichiometries and binding affinities.

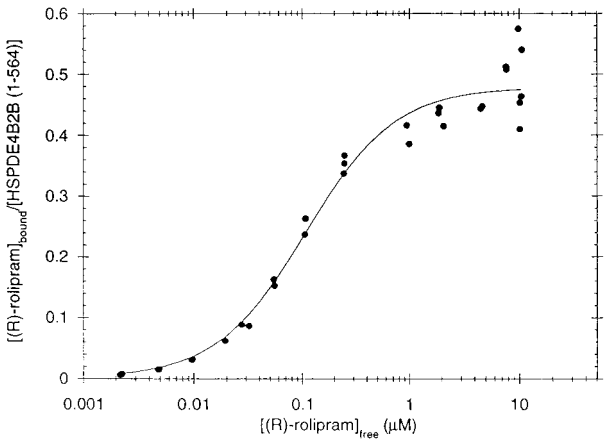

FIGURE 4: Typical (*R*)-rolipram binding isotherm of purified HSPDE4B2B 1−564 using equilibrium dialysis experiments. 5 μM HSPDE4B2B 1−564 protein was added to one side of a 200 μL (100 μL/side) dialysis chamber and 0.04−50 μM (*R*)-rolipram added to the other side. A specific radioactivity of 82 Ci/mmol was used for (*R*)-rolipram concentrations of 0.04−0.3 μM whereas a specific radioactivity of 0.33 Ci/mmol was used for (*R*)-rolipram concentrations >0.3 μM. The protein was dialyzed at 4 °C for 16 h. 50 μL samples were removed from each side of the chamber and counted in a 96-well microtiter plate. In most cases, duplicate or triplicate points were performed at each (*R*)-rolipram concentration. Data are plotted as $[\text{rolipram}]_{free}$ vs stoichiometry (n), $[\text{rolipram}_{bound}]/[\text{PDE}]$. A stoichiometry of 0.5 mol of (*R*)-rolipram per mole of HSPDE4B2B 1−564 was obtained with a K_d of 100 nM.

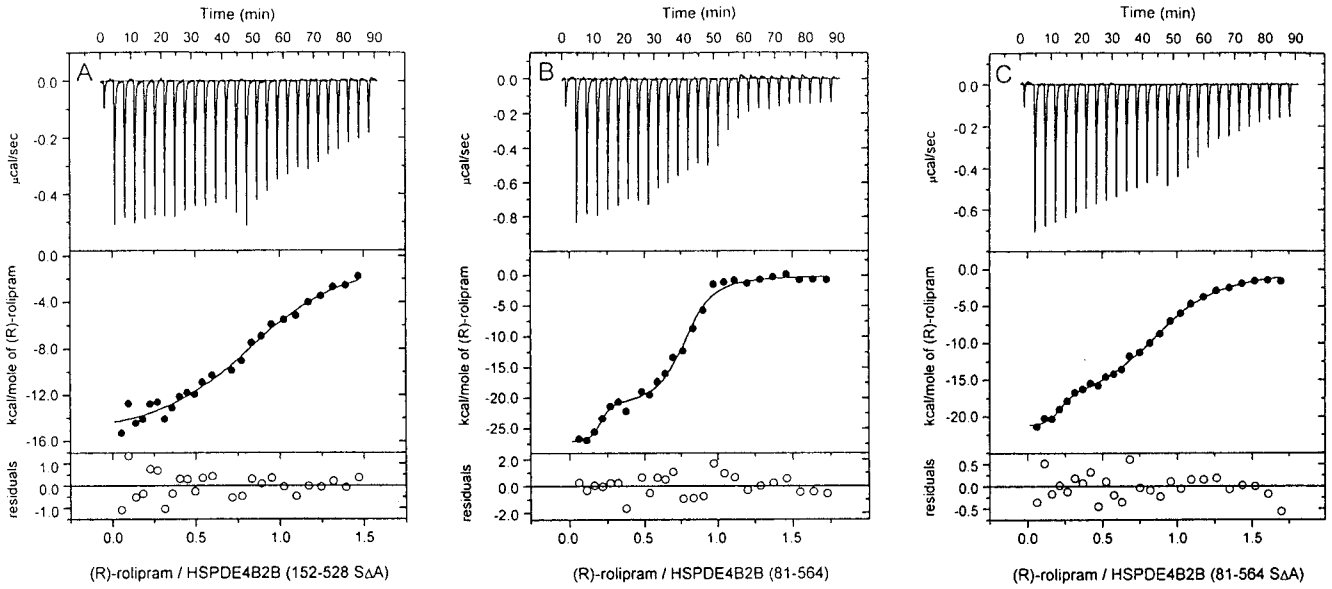

FIGURE 5: Examples of isothermal titration calorimetric data for the titration of (*R*)-rolipram into various purified HSPDE4B2B constructs. Top panels: 11 μM solutions of purified protein in 50 mM HEPES, 250 mM NaCl, 2 mM $MgCl_2$, and 0.5% DMSO, pH 7.5, were titrated with 100 μM (*R*)-rolipram in the same buffer. 27 injections were performed at 3.5 min intervals at a stirring speed of 600 rpm. An initial 2 μL injection was performed for each titration followed by the following injection schedule; 12, 8 μL injections; 7, 10 μL injections; and 7, 12 μL injections. (A) HSPDE4B2B 152−528 SΔA, (B) HSPDE4B2B 81−564, (C) HSPDE4B2B 81−564 SΔA. Middle panels: The area under each titration signal was integrated and plotted in the middle panel as a function of (*R*)-rolipram/HSPDE4B2B construct molar ratio. The solid line represents a nonlinear least-squares fit of the data assuming a single binding site for (A) and two independent binding sites for (B) and (C). The heat of dilution of (*R*)-rolipram into buffer was performed in a separate titration (not shown) and subtracted from the data before curve fitting. The fitting parameters K_b (association constant), *n*, and ΔH were determined from the best fit line. Bottom panels: The bottom panels show the difference between the raw data points and the fitted curve. Each titration was performed 3 times, and the results are shown in Table 3.

Binding of (R)-Rolipram to HSPDE4B2B Constructs Determined by Isothermal Titration Calorimetry. In order to better understand the stoichiometry of (*R*)-rolipram binding to HSPDE4B2B constructs, isothermal titration calorimetry (ITC) experiments were performed. ITC provides the thermodynamic parameters ΔG, ΔH, and ΔS; K_b (equilibrium binding constant); and stoichiometry (*n*) in a single experiment. The data obtained using ITC were consistent with data obtained using the other binding and kinetic techniques. The HSPDE4B2B 152−528 SΔA construct showed a single binding state for (*R*)-rolipram with a stoichiometry of 0.92 mol of (*R*)-rolipram per mole of enzyme and an apparent K_d of 1.0 μM (Figure 5A). The titrations of (*R*)-rolipram and HSPDE4B2B 152−528 SΔA were best fit to a single binding isotherm. The HSPDE4B2B 81−564 construct, however, showed two distinct binding states with apparent K_ds of 7.0 and 210 nM, indicating the existence of high- and low-affinity binding states, respectively (Figure 5B). The stoichiometry of (*R*)-rolipram binding to HSPDE4B2B 81−564 was 0.28 and 0.55 for high- and low-affinity states, respectively. Thus, the combined stoichiometry of 0.83 mol of (*R*)-rolipram per mole of HSPDE4B2B 81−564 suggests a single binding site in two different states; a low- and a high-affinity binding state. Consistent with the equilibrium dialysis stoichiometries, the data again suggest a single binding site, not two different binding sites, for (*R*)-rolipram.

The HSPDE4B2B 81−564 protein has been shown to be monophosphorylated at serine 487 and diphosphorylated at serine 487 and serine 489 at a 1:1 ratio (Lenhard et al., 1996). One possibility for the two different states (high- and low-affinity) is this phosphorylation. To determine whether or not phosphorylation was responsible for the two (*R*)-rolipram binding states, we used ITC to monitor (*R*)-rolipram binding to a dephosphorylated form of HSPDE4B2B 81−564, in which the serines at 482, 487, and 489 were mutated to alanines. When HSPDE4B2B 81−564 SΔA was analyzed by ITC, the data fit best to two binding states (Figure 5C). The stoichiometry for the high-affinity state was 0.26 mol of (*R*)-rolipram per mole of 81−564 SΔA, whereas the stoichiometry of the low-affinity state was 0.69 mol of (*R*)-rolipram per mole of 81−564 SΔA. The apparent K_d values for the high- and low-affinity states were 6.0 nM and 910 nM, respectively. The low-affinity state had a slightly higher observed binding constant than the wild-type 81−564 protein. This difference may be due to the phosphorylation. To date, ITC is the only technique that has provided unambiguous results as to the number of binding states for the HSPDE4B2B 81−564 SΔA protein. Filter binding data and (*R*)-rolipram inhibition data were ambiguous as to whether there was a single state or two different states for the HSPDE4B2B 81−564 SΔA protein.

Thermodynamics of (R)-Rolipram Binding to HSPDE4B2B Proteins As Measured by ITC. The relevant thermodynamic parameters of (*R*)-rolipram binding to HSPDE4B2B constructs are shown in Table 3. The total number of binding sites was ≤ 1 for each construct. The free energy for (*R*)-rolipram binding to the high- and low-affinity state of the nonphosphorylated HSPDE4B2B 81−564 was −11.3 and −8.3 kcal/mol, respectively. These free energies are composed of a large favorable enthalpic term of −20.2 and −17.3 kcal/mol for the high- and low-affinity states, respectively, with a large unfavorable entropic term. The free energy of binding to the dephosphorylated 81−564 protein was the same as the phosphorylated 81−564 protein in the high-affinity state, but 1 kcal/mol lower in the low-affinity state. The difference in binding enthalpies of the high- and low-affinity states was approximately 7 kcal/mol for the phosphorylated 81−564 protein at 16 or 28 °C, whereas the

Table 3: Thermodynamic Parameters of (*R*)-Rolipram Binding to Purified HSPDE4B2B Constructs As Determined by Isothermal Titration Calorimetry[a,b]

construct	binding affinity	stoichiometry (*n*)	$K_b \times 10^{-6}$ (M^{-1})	ΔH (kcal mol^{-1})	ΔG (kcal mol^{-1})	ΔS (eu)
81−564	high	0.28 ± 0.08	140 ± 98	−26.1 ± 2.3	−11.1 ± 0.4	−49.7 ± 8.5
	low	0.55 ± 0.07	4.8 ± 0.4	−18.8 ± 1.6	−9.2 ± 0.04	−34.1 ± 6.3
81−564 SΔ	high	0.26 ± 0.08	164 ± 74	−20.2 ± 1.6	−11.3 ± 0.3	−29.6 ± 5.6
	low	0.69 ± 0.02	1.1 ± 0.3	−17.3 ± 1.4	−8.3 ± 0.2	−29.8 ± 5.0
152−528 SΔA	high	NA[c]	NA	NA	NA	NA
	low	0.92 ± 0.08	1.0 ± 0.6	−16.0 ± 0.8	−8.2 ± 0.3	−25.8 ± 3.6

[a] All experiments were performed at 28 °C. [b] The standard errors presented are from three separate titrations. [c] NA, not applicable.

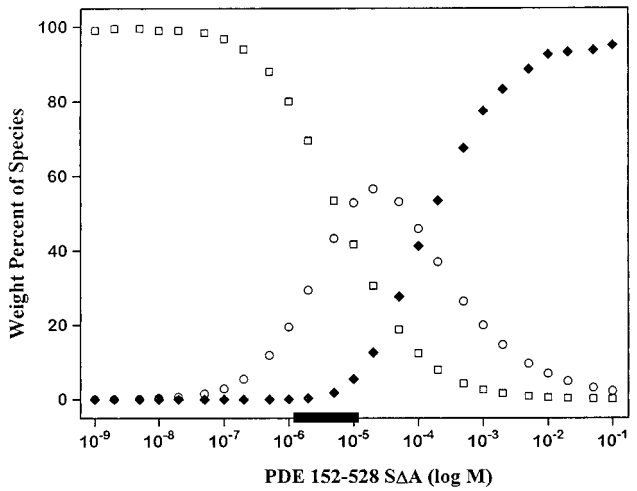

FIGURE 6: Calculated weight fraction distribution of monomer−dimer−tetramer species vs log of molar HSPDE4B2B 152−528 SΔA concentration. Equilibrium constants, converted to molar dissociation constants, were used to calculate theoretical concentrations of monomer, dimer, and tetramer. □ denotes % monomer. ○ denotes % dimer. ◆ denotes % tetramer. The mean of multiple equilibrium constants at 4 °C, 20 000 rpm, was used to create this representation. The bar denotes the experimental concentration range (2−20 μM) within which ultracentrifugation data were collected.

difference in binding enthalpies was only 3 kcal/mol for the dephosphorylated 81−564 protein. These data suggest only slight differences in (*R*)-rolipram binding to the phosphorylated and nonphosphorylated proteins. Similar to other binding data presented, no high-affinity binding was detected in the 152−528 dephosphorylated protein; however, the free energy of binding (−8.2 kcal/mol) was consistent with binding to the low-affinity state. Reducing the temperature from 28 to 16 °C decreased the low-affinity binding constant of the 81−564 protein by almost 4-fold but decreased the high-affinity binding constant <2-fold (data not shown). The significance of this finding, if any, is unknown at the present time.

Determination of HSPDE4B2B Construct Association State by Equilibrium Ultracentrifugation. To determine the native association state of each HSPDE4B2B construct, analytical equilibrium ultracentrifugation studies were performed. At the concentrations examined, HSPDE4B2B 81−564 migrated as a self-associating complex in solution, but when the data were fit to monomer/dimer, dimer, monomer/trimer, and monomer/tetramer association models, the results appeared statistically indistinguishable. The apparent K_d of the monomer/*n*-mer complex was 10−20 μM (data not shown).

In comparison, at concentrations of protein above 1 μM, HSPDE4B2B 152−528 SΔA had a clear propensity to associate as dimers (Figure 6). The K_d of the monomer/dimer complex was 20 μM. At protein concentrations above 20 μM, the enzyme begins to form tetramers in solution. The region of amino acids (152−528), therefore, is responsible for regular self-association into dimer and tetramer complexes. Also, the data would suggest that under the conditions used for titration calorimetry and equilibrium dialysis experiments (11 μM and 5 μM, respectively), an appreciable amount of dimer was present; however, no high-affinity (*R*)-rolipram binding was detected in the titration calorimetry experiments. Under the conditions of the filter binding and kinetic experiments (10 nM and 1 nM, respectively), the 152−528 SΔA protein existed in a monomeric form. These results suggest that protein self-association is not directly responsible for high-affinity (*R*)-rolipram binding. HSPDE4B2B 152−528 SΔA showed no high-affinity binding in filter binding or ITC experiments, yet is in different oligomeric states in these assays. Additional studies using dynamic light scattering also showed that HSPDE4B2B 152−528 SΔA is a self-associating system and that equal molar concentrations of (*R*)-rolipram produce no additional protein association (data not shown). The presence of phosphate moieties on serines 487 and 489 had no significant effect on the association state of the 152−528 construct (data not shown).

When HSPDE4B2B 1−564 was analyzed by ultracentrifugation, the protein migrated with >30 HSPDE4B2B 1−564 protein molecules per unit. Unlike the 152−528 SΔA and 81−564 proteins, the association state of 1−564 during kinetic and filter binding assays could not be extrapolated. However, gel filtration studies at the nanomolar protein concentrations used in filter binding and kinetic studies still show the HSPDE4B2B 1−564 protein migrates as a large multimer (data not shown). These results suggest the 1−564 protein self-associates under the conditions of high-affinity (*R*)-rolipram kinetic and binding assays.

DISCUSSION

Two Type 4 phosphodiesterases, HSPDE4A and HSPDE4B2B, have been cloned from human brain and expressed in recombinant systems (McLaughlin et al., 1993; Livi et al., 1990). Data from these studies suggest that these proteins contain a high-affinity (*R*)-rolipram binding site that may represent an allosteric site or one of two distinct catalytic forms of the protein molecule (Torphy et al., 1992). In the past, it has been proposed that there could be two different rolipram binding sites on Type 4 PDEs: a high-affinity site, responsible for the pharmacological effects of rolipram; and a catalytic site, responsible for enzyme inhibition (Torphy et al., 1992; Nemoz et al., 1989). Recently, Jacobitz et al. (1996) reported that HSPDE4A may contain a high-affinity rolipram binding site within amino acids 265−332 of the protein, which is outside the catalytic domain. As an alternative, they suggest these residues are required for a

conformation that binds rolipram at the catalytic site with high-affinity.

To eliminate any speculation of other proteins or cellular factors interfering with our analyses, we performed our studies with purified proteins. From a baculovirus expression system, we have purified to homogeneity HSPDE4B2B 81−564 and 152−528 protein constructs to determine the stoichiometry of (*R*)-rolipram binding, the site(s) of binding, and the role of HSPDE4B2B phosphorylation in the (*R*)-rolipram binding and inhibition kinetics. Where possible, we have compared these results to the purified full-length HSPDE4B2B 1−564 protein. These studies were undertaken in an attempt to understand the physical nature of (*R*)-rolipram binding to HSPDE4B2B and to assist in designing better isozyme specific inhibitors of the enzyme.

The expressed and purified proteins all exhibited similar K_m values for cAMP with specific activities ranging from 10 to 40 μmol min^{-1} (mg of protein)$^{-1}$. The HSPDE4B2B 1−564 protein appeared 3−4-fold less active (k_{cat}/K_m) than the rest of the isolated HSPDE4B2B enzymes. The kinetic results with HSPDE4B2B 1−564 correlate well with those reported on the analogous rat PDE3 protein (Jin et al., 1992) in which a deletion of the first 97 amino acid residues increased activity 3-fold. Removing the first 80 amino acids from HSPDE4B2B results in a self-associating protein, significantly less oligomeric than HSPDE4B2B (1−564), suggesting a key role for the N-terminal domain (1−80) in regulating HSPDE4B2B. This N-terminal domain is not conserved among the different isoforms of Type 4 PDEs, and therefore could be responsible for the specificity of action. Attempts to express and purify amino acids 1−80 in *E. coli* to determine if this domain self-associates and/or interacts with other proteins in the cell have been unsuccessful to date.

After each protein was purified and exact protein concentrations were determined from quantitative amino acid analyses, experiments were initiated to determine the stoichiometry of (*R*)-rolipram binding to the various HSPDE4B2B proteins. Kinetic, filter binding, equilibrium dialysis, and titration calorimetry experiments were set up to determine if there was one or two binding sites for (*R*)-rolipram on HSPDE4B2B. In all the assays tested, the stoichiometry of (*R*)-rolipram binding to HSPDE4B2B was never >1 mol of (*R*)-rolipram per mole of protein, suggesting only a single (*R*)-rolipram binding site on the enzyme. The longer HSPDE4B2B constructs, 1−564 and 81−564, bound (*R*)-rolipram with both high-affinity (∼7 nM) and low-affinity (>100 nM), whereas the shorter HSPDE4B2B 152−528 protein only bound (*R*)-rolipram with low-affinity. (*R*)-Rolipram binding to the low-affinity state is rapid and does not require preincubation of enzyme with inhibitor. The apparent K_d for (*R*)-rolipram binding that we observe is similar to the apparent K_i for enzyme inhibition previously observed by others (Bolger et al., 1993; Nemoz et al., 1989); therefore, it is likely that this represents binding of (*R*)-rolipram in the catalytic site of the enzyme. Only when the HSPDE4B2B 1−564 and 81−564 proteins are preincubated with (*R*)-rolipram for 1 h do we detect enzyme inhibition around 5 nM. These results also suggest that high-affinity (*R*)-rolipram binding represents binding to the catalytic site of the protein. Thus, it appears from the kinetic data that there exists a single binding site for (*R*)-rolipram (i.e., the catalytic site) which can exist in at least two forms, one binding (*R*)-rolipram with high-affinity and the other binding with lower affinity. For the HSPDE4B2B 152−528 protein, the (*R*)-rolipram inhibition profiles were similar in the presence or absence of preincubation. One possible reason why the truncated HSPDE4B2B 152−528 protein is not inhibited at low nanomolar (*R*)-rolipram concentrations is that the protein lacks the conformation necessary to bind (*R*)-rolipram with high-affinity. If this hypothesis is correct, it may indicate that amino acid residues in the N-terminus (81−151) and/or C-terminus (529−564) are required, along with the conserved catalytic region (152−528), to bind (*R*)-rolipram with high-affinity.

To further dissect the residues necessary for high-affinity binding, we expressed amino acid residues 81−528 in Sf9 cells. A partially purified preparation of this protein also bound (*R*)-rolipram with high-affinity, suggesting that amino acids in the N-terminus (81−151) and catalytic domain (152−528) are responsible for high-affinity (*R*)-rolipram binding, whereas residues in the catalytic domain itself are sufficient for low-affinity binding. These results are consistent with those suggested by Jacobitz et al. (1996) for HSPDE4A, in that HSPDE4A (amino acids 265−886; corresponding to amino acids 81-carboxy terminus of HSPDE4B2B) bound rolipram with high- and low-affinity but HSPDE4A (amino acids 332−886; corresponding to residues 133-carboxy terminus of HSPDE4B2B) only bound rolipram with low-affinity.

The lack of high-affinity (*R*)-rolipram binding in the HSPDE4B2B 152−528 protein was further corroborated by titration calorimetry experiments. The HSPDE4B2B 152−528 SΔA protein always showed a single binding state, whereas the longer protein, 81−564, showed two distinct binding forms. Due to the large oligomeric properties of the HSPDE4B2B 1−564 protein and quantities of protein necessary for multiple experiments, we were unable to obtain accurate calorimetric information on this construct. Since HSPDE4B2B 81−564 showed similar high- and low-affinity binding and inhibition properties as the 1−564 protein, we felt HSPDE4B2B 81−564 was a suitable substitute for the full-length protein. The cumulative stoichiometry of high- and low-affinity (*R*)-rolipram binding was ≤1 for each of the proteins tested in the titration calorimetry experiments. Furthermore, the equilibrium between the high- and low-affinity conformation appears to favor the low-affinity state under the titration calorimetry conditions, since the ratio of the low-affinity stoichiometry to the high-affinity stoichiometry was always ≥2:1. Again, from these results, we conclude that a single (*R*)-rolipram binding site exists on the protein. This site is able to exist in two different states, one binding (*R*)-rolipram with high-affinity and another binding (*R*)-rolipram with low-affinity. The conformational state of the N-terminus and catalytic domain that allows (*R*)-rolipram to bind with high-affinity is unknown.

One could imagine that the N-terminal domain 81−151 and catalytic domain 152−528 allow for high-affinity (*R*)-rolipram binding through protein self-association or the phosphorylation state of the protein. The HSPDE4B2B 81−564 and 152−528 SΔA proteins appear to be monomeric at the concentrations used for kinetic studies and filter binding assays but both monomeric and dimeric at concentrations used for titration calorimetry experiments. The results from binding and kinetic experiments showed high-affinity (*R*)-rolipram binding to the HSPDE4B2B 81−564 protein but

no high-affinity (*R*)-rolipram binding to the 152−528 SΔA protein. Thus, it does not appear that dimerization of the protein is responsible for the observed high-affinity (*R*)-rolipram binding state. What still remains clear is that high-affinity (*R*)-rolipram binding only occurs when amino acid residues 81−151 and amino acids in the catalytic domain (152−528) are expressed on the same protein.

To further investigate whether phosphorylation affects high- and low-affinity (*R*)-rolipram binding, kinetic and titration calorimetry experiments were performed. Given that there are at least two populations of HSPDE4B2B in each construct due to mono- and diphosphorylated species (Lenhard et al., 1996), we constructed mutant proteins in which the serines at residues 482, 487, and 489 were replaced with alanine. The change in free energy (ΔG) of the phosphorylated and dephosphorylated HSPDE4B2B 81−564 high-affinity binding state (−11.1 and −11.3 kcal/mol, respectively) as measured by titration calorimetry was remarkably similar to that reported from van't Hoff plots of soluble brain PDE (−11.9 kcal/mol; Schneider et al., 1986). Kinetic and filter binding data were ambiguous as to whether a high-affinity binding state existed on the HSPDE4B2B 81−564 SΔA dephosphorylated protein, but titration calorimetry results clearly indicated the presence of a high-affinity binding state. The concentrations of protein used for titration calorimetry experiments were 100−1000 times higher then the concentrations used for the kinetics and filter binding assays. Since the concentration of protein is the only major variable between the assays, the protein concentration may somehow affect the high-affinity binding in the dephosphorylated HSPDE4B2B 81−564 protein. Since no high-affinity (*R*)-rolipram binding was detected in the HSPDE4B2B 152−528 SΔA protein but high-affinity (*R*)-rolipram binding was detected with the 81−564 SΔA protein, phosphorylation does not appear to be solely responsible for high-affinity (*R*)-rolipram binding. Until a three-dimensional structure of the 81−564 enzyme is obtained in the presence of (*R*)-rolipram, these speculations concerning (*R*)-rolipram binding interactions may remain unanswered.

Finally, although data exist for high-affinity (*R*)-rolipram binding to HSPDE4B2B, information regarding the stoichiometry has never been reported due to the lack of purity and low recoveries of the Type 4 PDE proteins. Our data indicate that purified HSPDE4B2B 1−564 and 81−564 contain a single binding site (i.e., the active site) for (*R*)-rolipram with two affinities. The high-affinity binding state of the protein requires the interaction of amino acid residues at the N-terminus (81−151) and catalytic domain (152−528) of the protein, whereas the low-affinity binding state only requires residues in the catalytic domain. Phosphorylation at residues 487 and 489 of the protein does not appear to alter the stoichiometry or binding affinity of (*R*)-rolipram but may shift the equilibrium of (*R*)-rolipram binding. Furthermore, the regular association state of the purified proteins does not appear to affect (*R*)-rolipram binding. From these results, we have been able to design isozyme specific inhibitors that bind to the catalytic site only with high-affinity ($\leq$1 nM) and with a stoichiometry of 1 mol of inhibitor per mole of protein. We are presently pursuing the structure of various HSPDE4B2B constructs and examining other truncation and deletion mutants to determine specific residues responsible for high-affinity (*R*)-rolipram binding.

ACKNOWLEDGMENT

We thank Mary Moyer and Will Burkhart for amino acid analysis and Edman sequencing results. We thank Dan Kassel for his mass spectrometry results and Tom Consler for his analytical ultracentrifugation results. Finally, we especially thank Tim Martins and Vince Florio from the ICOS Corp. in Bothell, WA, for supplying purified HSPDE4B2B 1−564 for our biochemical studies.

REFERENCES

Amegadzie, B. Y., Hanning, C. R., McLaughlin, M. M., Burman, M., Cieslinski, L. B., Livi, G. P., & Torphy, T. J. (1995) *Cell Biol. Int. 19*, 477−484.

Beavo, J. A. (1988) in *Advances in Second Messenger and Phosphoprotein Research* (Greengard, P., & Robison, G. A., Eds.) Vol. 22, pp 1−38, Raven Press, New York.

Beavo, J. A., & Reifsnyder, D. H. (1990) *Trends Pharmacol. Sci. 11*, 150−155.

Bolger, G., Michaeli, T., Martins, T., St. John, T., Steiner, B., Rodgers, L., Riggs, M., Wigler, M., & Ferguson, K. (1993) *Mol. Cell. Biol. 13*, 6558−6571.

Bourne, H. R., Lichtenstein, L. M., Melmon, K. L., Henney, C. S., Weinstein, Y., & Shearer, G. M. (1974) *Science 184*, 19−28.

Cantor, C. R., & Schimmel, P. P. (1980) *Biophysical Chemistry Part III: The Behavior of Biological Macromolecules*, W. H. Freeman and Co., New York.

Cleland, W. W. (1970) in *The Enzymes* (Boyer, P. D., Ed.) Vol. 2, p 56, Academic Press, New York.

Cohn, E. J., & Edsall, J. T. (1943) *Proteins, amino acids and peptides as ions and dipolar ions*, p 157, Rheinhold, New York.

Durschlag, H. (1986) *Thermodynamic data for biochemistry and biotechnology* (Hinz, H. J., Ed.) p 45, Springer-Verlag, New York.

Jacobitz, S., McLaughlin, M. M., Livi, G. P., Burman, M., & Torphy, T. J. (1996) *Mol. Pharmacol. 50*, 891−899.

Jin, S.-L. C., Swinnen, J. V., & Conti, M. (1992) *J. Biol. Chem. 267*, 18929−18939.

Klotz, I. M., Walker, F. W., & Pivan, R. B. (1946) *J. Am. Chem. Soc. 68*, 1486−1490.

Laue, T. M., Shah, B. D., Ridgeway, T. M., & Pelletier, S. L. (1992) *Analytical ultracentrifugation in biochemistry and polymer science* (Harding, S. E., Rowe, A. J., & Horton, J. C., Eds.) p 102, The Royal Society of Chemistry, Cambridge.

Lenhard, J. M., Kassel, D. B., Rocque, W. J., Hamacher, L., Holmes, W. D., Patel, I., Hoffman, C., & Luther, M. A. (1996) *Biochem. J. 316*, 751−758.

Lin, L.-N., Mason, A. B., Woodworth, R. C., & Brandts, J. F. (1991) *Biochemistry 30*, 11660−11669.

Livi, G. P., Kmetz, P., McHale, M. M., Cieslinski, L. B., Sathe, G. M., Taylor, D. P., Davis, R. L., Torphy, T. J., & Balcarek, J. M. (1990) *Mol. Cell. Biol. 10*, 2678−2686.

Marquardt, D. W. (1963) *J. Soc. Ind. Appl. Math. 11*, 431−441.

McLaughlin, M. M., Cieslinski, L. B., Burman, M., Torphy, T. J., & Livi, G. P. (1993) *J. Biol. Chem. 268*, 6470−6476.

McRorie, D. K., & Voelker, P. J. (1993) *Self-Associating Systems in the Analytical Centrifuge*, pp 13−23, Beckman Instruments Inc., Fullerton, CA.

Michaeli, T., Bloom, T. J., Martins, T., Loughney, K., Ferguson, K., Riggs, M., Rodgers, L., Beavo, J. A., & Wigler, M. (1993) *J. Biol. Chem. 268*, 12925−12932.

Nemoz, G., Moueqqit, M., Prigent, A. F., & Pacheco, H. (1989) *Eur. J. Biochem. 184*, 511−520.

Nicholson, C. D., Shahid, M., vanAmsterdam, R. G. M., & Zaagsma, J. (1990) *Eur. J. Pharmacol. 183*, 1097−1098.

Obernolte, R., Bhakta, S., Alvarez, R., Bach, C., Zuppan, P., Mulkins, M., Jarnagin, K., & Shelton, E. R. (1993) *Gene 129*, 239−247.

O'Reilly, D. R., Miller, L. K., & Luckow, V. A. (1992) *Baculovirus expression vectors. A laboratory manual*, W. H. Freeman, New York.

Pillai, R., Kytle, K., Reyes, A., & Colicelli, J. (1993) *Proc. Natl. Acad. Sci. U.S.A. 90*, 11970−11974.

Rocque, W. J., Holmes, W. D., Patel, I. R., Dougherty, R. W., Ittoop, O., Overton, L., Hoffman, C. R., Wisely, G. B., Willard, D. H., & Luther, M. A. (1997) *Protein Expression Purif. 9*, 191−202.

Schneider, H. H., Schmiechen, R., Brezinski, M., & Seidler, J. (1986) *Eur. J. Pharmacol. 127*, 105−115.

Silver, P. J., Hammel, L. T., Perrone, M. H., Bentley, R. G., Bushover, C. R., & Evans, D. B. (1988) *Eur. J. Pharmacol. 150*, 85−94.

Summers, M. D., & Smith, G. E. (1987) *A manual of methods for baculovirus vectors and insect cell culture procedures*, Texas Agricultural Experiment Station Bulletin, p 1555.

Torphy, T. J., & Cieslinski, L. B. (1990) *Mol. Pharmacol. 37*, 206−214.

Torphy, T. J., & Hay, D. W. P. (1990) in *Airway smooth muscle: modulation of receptors and response* (Townley, R. G., & Argrawal, D. K., Eds.) pp 39−68, CRC Press, Boca Raton.

Torphy, T. J., & Undem, B. J. (1991) *Thorax 46*, 512−523.

Torphy, T. J., Stadel, J. M., Burman, M., Cieslinski, L. B., McLaughlin, M. M., White, J. R., & Livi, G. P. (1992) *J. Biol. Chem. 267*, 1798−1804.

Wiseman, T., Williston, S., Brandts, J. F., & Lin, L.-N. (1989) *Anal. Biochem. 179*, 131−137.

BI971112E